Measurement of *CP*-Violating and Mixing-Induced Observables in $B_s^0 \to \phi\gamma$ Decays

R. Aaij *et al.*[*]
(LHCb Collaboration)

(Received 20 May 2019; published 23 August 2019)

A time-dependent analysis of the $B_s^0 \to \phi\gamma$ decay rate is performed to determine the CP -violating observables $S_{\phi\gamma}$ and $C_{\phi\gamma}$ and the mixing-induced observable $\mathcal{A}^{\Delta}_{\phi\gamma}$. The measurement is based on a sample of pp collision data recorded with the LHCb detector, corresponding to an integrated luminosity of 3 fb^{-1} at center-of-mass energies of 7 and 8 TeV. The measured values are $S_{\phi\gamma} = 0.43 \pm 0.30 \pm 0.11$, $C_{\phi\gamma} = 0.11 \pm 0.29 \pm 0.11$, and $\mathcal{A}^{\Delta}_{\phi\gamma} = -0.67^{+0.37}_{-0.41} \pm 0.17$, where the first uncertainty is statistical and the second systematic. This is the first measurement of the observables S and C in radiative B_s^0 decays. The results are consistent with the standard model predictions.

DOI: 10.1103/PhysRevLett.123.081802

In the standard model (SM) of particle physics, the $b \to s\gamma$ transition proceeds via loop Feynman diagrams. The small size of the SM amplitude makes such a process sensitive to the contribution of possible new particles. The emitted photons are produced predominantly with left-handed helicity in the SM due to parity violation in the weak interaction, with a small relative right-handed component proportional to the ratio of s- to b-quark masses. In many extensions of the SM, the right-handed component can be enhanced, leading to observable effects in mixing-induced CP asymmetries and time-dependent decay rates of radiative B^0 and B_s^0 decays [1–3]. Current measurements sensitive to right-handed contributions [4–9] are in agreement with SM predictions [10].

The rate $\mathcal{P}(t)$ at which B_s^0 or $\bar{B}_s^0$ mesons decay to a common final state that contains a photon, such as $\phi\gamma$ [where ϕ refers to $\phi(1020)$], depends on the decay time t as [3]

$$\mathcal{P}(t) \propto e^{-\Gamma_s t}\{\cosh(\Delta\Gamma_s t/2) - \mathcal{A}^{\Delta}\sinh(\Delta\Gamma_s t/2) + \zeta C\cos(\Delta m_s t) - \zeta S\sin(\Delta m_s t)\}, \quad (1)$$

where $\Delta\Gamma_s$ and Δm_s are the width and mass differences between the B_s^0 mass eigenstates, respectively, defined positively, Γ_s is the mean decay width between such eigenstates, and ζ takes the value of $+1$ (-1) for an initial B_s^0 $(\bar{B}_s^0)$ state. The coefficients $\mathcal{A}^{\Delta}$ and S are sensitive to the photon helicity amplitudes and weak phases, while C is related to CP violation in the decay. The SM predictions for the three coefficients in the $B_s^0 \to \phi\gamma$ decay are close to zero [3]. The LHCb Collaboration has previously measured $\mathcal{A}^{\Delta}_{\phi\gamma} = -0.98^{+0.46}_{-0.52}{}^{+0.23}_{-0.20}$ [9] from a time-dependent flavor-untagged analysis, which is compatible with the SM within 2 standard deviations.

This Letter reports the first measurement of the CP-violating observables S and C from a radiative B_s^0 decay, determined from the time-dependent rate of $B_s^0 \to \phi\gamma$ decays in which the ϕ meson decays to a K^+K^- pair. An update of the $\mathcal{A}^{\Delta}_{\phi\gamma}$ coefficient measurement is also provided. Results are based on data collected with the LHCb detector in pp collisions at center-of-mass energies of 7 and 8 TeV during the years 2011 and 2012, respectively, corresponding to an integrated luminosity of 3 fb^{-1}. Compared to Ref. [9], the current analysis benefits from a 20% higher event selection efficiency, a reoptimized calorimeter reconstruction, and a new photon identification algorithm. Flavor-tagging algorithms are applied to determine the initial flavor of the B_s^0 or $\bar{B}_s^0$ meson, which is essential to measure the S and C observables, whereas flavor-untagged decays still contribute to the measurement of $\mathcal{A}^{\Delta}$. The background is subtracted from a fit to the mass distribution of the B_s^0 candidates. A sample of untagged $B^0 \to K^{*0}\gamma$ decays [where K^{*0} refers to $K^{*0}(892)$], reconstructed in the flavor-specific $K^{*0} \to K^+\pi^-$ final state, is used to control the decay-time-dependent efficiency, since its lifetime is well measured. Throughout this Letter, the inclusion of charge-conjugated processes is implied.

The LHCb detector is a single-arm forward spectrometer covering the pseudorapidity range $2 < \eta < 5$, described in detail in Refs. [11,12]. It includes a high-precision tracking system consisting of a silicon-strip vertex detector surrounding the pp interaction region, a large-area silicon-strip detector located upstream of a dipole magnet with a bending power of about 4 Tm, and three stations of silicon-strip

[*]Full author list given at the end of the article.

detectors and straw drift tubes placed downstream of the magnet. Different types of charged hadrons are distinguished using information from two ring-imaging Cherenkov detectors. Photons, electrons, and hadrons are identified by a calorimeter system consisting of scintillating-pad and preshower detectors and an electromagnetic and a hadronic calorimeter.

The online event selection is performed by a trigger system, which consists of a hardware stage, based on information from the calorimeter and muon systems, followed by a software stage, which applies a full event reconstruction. Two trigger selections are defined, with different photon and track momentum thresholds. Samples of simulated events, produced with the software described in Refs. [13–18], are used to characterize signal and background contributions. The signal sample is generated with the three coefficients $\mathcal{A}^{\Delta}_{\phi\gamma}$, $C_{\phi\gamma}$, and $S_{\phi\gamma}$ set to zero.

Candidate $B^0_s \to \phi\gamma$ decays are reconstructed from a photon candidate and two oppositely charged particles identified as kaons. The selection is designed to maximize the significance $S/\sqrt{S+B}$ of the signal yield. Photons are reconstructed from energy deposits in the electromagnetic calorimeter and required to have a momentum transverse to the beam axis, p_T, larger than 3.0 or 4.2 GeV/c, depending on the trigger selection. Background due to photons from π^0 decays is rejected by a dedicated algorithm [19]. The kaon candidates are required to have $p > 1.0$ GeV/c and $p_T > 0.3$ GeV/c, where p is the total momentum, and at least one of them must fulfill $p > 10$ GeV/c and $p_T > 1.2$ or 1.8 GeV/c, depending on the trigger selection. Kaon candidates are required to be inconsistent with originating from a primary pp interaction vertex and must form a common vertex of good quality. The K^+K^- system must have an invariant mass within 15 MeV/c^2 of the known ϕ mass [20]. The B^0_s candidate must be consistent with originating from only one pp interaction vertex, and only candidates with decay times between 0.3 and 10 ps are retained. In addition, the cosine of the helicity angle (θ_H), defined as the angle between the momenta of the positively charged kaon and that of the B^0_s meson in the rest frame of the ϕ meson, is required to be less than 0.8 in absolute value. This requirement helps to suppress the π^0 and combinatorial backgrounds, which are expected to be distributed as $\cos^2\theta_H$ and a uniform distribution, respectively, as opposed to the $\sin^2\theta_H$ distribution expected for the signal. The $B^0 \to K^{*0}\gamma$ decay, with $K^{*0} \to K^+\pi^-$, is selected with almost identical requirements. A pion is required instead of a kaon, and the invariant mass of the $K^+\pi^-$ system must be within 100 MeV/c^2 of the known K^{*0} mass [20].

The signal yields are 5110 ± 90 for $B^0_s \to \phi\gamma$ decays and 33860 ± 250 for $B^0 \to K^{*0}\gamma$ decays, where the uncertainties are statistical only. They are obtained from separate extended unbinned maximum-likelihood fits to the

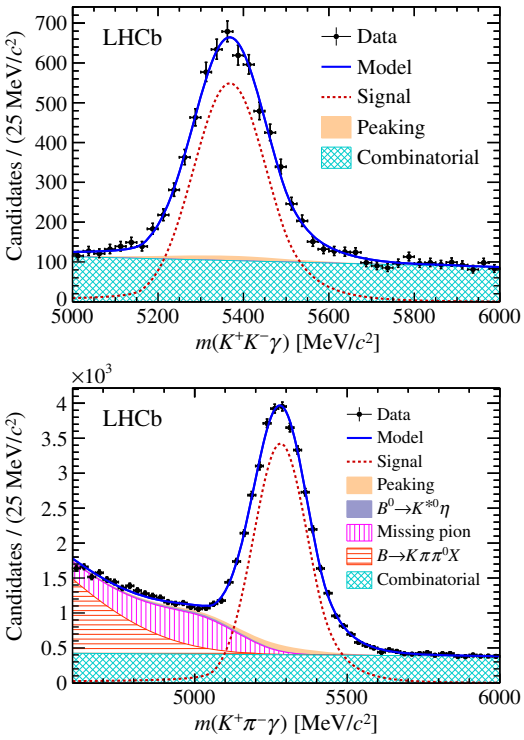

FIG. 1. Fits to the mass distributions of the (top) $B^0_s \to \phi\gamma$ and (bottom) $B^0 \to K^{*0}\gamma$ candidates.

$B^0_s \to \phi\gamma$ and $B^0 \to K^{*0}\gamma$ reconstructed mass distributions in the ranges 5000–6000 and 4600–6000 MeV/c^2, respectively. The mass fits are shown in Fig. 1. The results are used to assign weights to the candidates in the data samples in order to subtract the backgrounds [21]. The signal line shapes are described by modified Crystal Ball functions [22], consisting of a Gaussian core with power-law tails on both sides of the peak. The mean and width of the Gaussian core are obtained from the data, while the tail parameters are determined from the simulation. Three background categories are considered: combinatorial, peaking, and partially reconstructed. The combinatorial background, modeled by a linear function, is produced by the wrong association of a random photon with two hadrons mostly coming from real ϕ and K^{*0} resonances. The peaking backgrounds originate from other b-hadron decays with a reconstructed mass falling under the signal peak, due to the misidentification of one or several final-state particles. All possible combinations of misidentified hadrons, or the misidentification of a π^0 meson as a photon, are considered for the signal and control decay channels. For the $B^0_s \to \phi\gamma$ decay channel, the relevant contributions are $B^0_s \to \phi\pi^0$ and $\Lambda^0_b \to (pK^-)\gamma$, where pK^- comes from $\Lambda(1520)$ and further baryon resonances. For the $B^0 \to K^{*0}\gamma$ decay channel, the $B^0 \to K^{*0}\pi^0$ and $\Lambda^0_b \to (pK^-)\gamma$ decays are taken into account. Each peaking background is modeled with a Crystal Ball function. The shape parameters are

determined from the simulation, except for the width of the Gaussian core, which is multiplied by a factor to account for the difference in resolution between the data and simulation. The yield ratios of peaking backgrounds to the signal are calculated using simulation samples and taking the branching ratios from experimental measurements [6,9]. They are determined to be below 2% in all cases. Partially reconstructed backgrounds originate from other b-hadron decays in which one or several final-state particles are not reconstructed. This contribution is negligible in $B_s^0 \to \phi\gamma$ decays, while for the $B^0 \to K^{*0}\gamma$ mode the dominant contributions are decays of the type $B \to K\pi\pi\gamma$ with a missing pion, decays of the type $B \to K\pi\pi^0 X$ (mainly from $B^+ \to \bar{D}^0\rho^+$ decays) with one or several missing hadrons, and $B^0 \to K^{*0}\eta(\gamma\gamma)$ decays with a missing photon. They are described by an ARGUS function [23] convolved with a Gaussian function to account for the detector resolution, with the shape parameters determined from simulation.

Flavor-tagging algorithms are applied to identify the initial flavor of the B_s^0 meson. They provide a tag decision q, which takes the value $+1$ if the signal was originally a B_s^0 meson, -1 if it was a $\bar{B}_s^0$ meson, and zero if no decision is given. The algorithms also provide an estimate η of the probability for the tag decision to be incorrect (mistag probability). Two classes of flavor-tagging algorithms are used: same-side (SS) [24] and opposite-side (OS) taggers [25]. The SS tagger determines the flavor of the signal candidate by identifying the charge of the kaon produced together with the B_s^0 meson in the fragmentation process and is based on a neural network algorithm [24]. The OS taggers rely on the pair production of b hadrons in pp collisions and examine the decay products of the other b hadron in the event. The information used includes the charge of the leptons produced in semileptonic decays, the charge of kaons produced in $b \to c \to s$ transitions, and the charge of the particles originating from the decay vertex [25].

The mistag probability estimate η is calibrated using a linear function to obtain a corrected mistag probability ω for the signal sample. This is performed using mainly samples of $B^+ \to J/\psi K^+$ and $B^0 \to J/\psi K^{*0}$ decays for the OS tagger and $B_s^0 \to D_s^-\pi^+$ and $B_{s2}^*(5840)^0 \to B^+K^-$ decays for the SS tagger. The uncertainties of the calibration parameters include a systematic uncertainty that takes into account possible differences of these parameters between the decays used for calibration and other B-decay modes. The validity of these calibrations for $B_s^0 \to \phi\gamma$ decays is checked using both the simulation and data. Finally, the outputs of the algorithms are combined into a single decision and mistag probability. The effective tagging efficiency $\epsilon_{\text{eff}} = (4.99 \pm 0.14)\%$ is the product of the probability to obtain a decision $\epsilon_{\text{tag}} = (74.5 \pm 0.8)\%$ and the square of the effective dilution $D = 1\text{–}2\omega = (25.9 \pm 0.3)\%$.

The CP -violating and mixing-induced observables are determined from a weighted unbinned maximum-likelihood fit [26] to the decay-time distributions, performed simultaneously on the $B_s^0 \to \phi\gamma$ and $B^0 \to K^{*0}\gamma$ samples. The signal probability density function (PDF) of the $B_s^0 \to \phi\gamma$ decay-time distribution is defined as the decay rate $\mathcal{P}(t)$ in Eq. (1), convolved with a resolution function and multiplied by a decay-time-dependent efficiency $\epsilon(t)$. For the $B^0 \to K^{*0}\gamma$ decay, the time-dependent decay rate is described as a single exponential function. The physics parameters are constrained to the averages from Ref. [27]: $\tau_{B^0} = 1.520 \pm 0.004$ ps, $\Gamma_s = 0.6629 \pm 0.0018$ ps^{-1}, $\Delta\Gamma_s = 0.088 \pm 0.006$ ps^{-1}, and $\Delta m_s = 17.757 \pm 0.021$ ps^{-1}. The correlation of -0.11 between the Γ_s and $\Delta\Gamma_s$ parameters is taken into account.

The decay-time resolution is modeled by the sum of two Gaussian functions, with a common mean and independent widths. The widths are given by the per-candidate decay-time uncertainties, multiplied by constant scaling factors determined from the simulation to account for an observed underestimation of the uncertainties. Additional control samples are used to determine the decay-time resolution differences between the simulation and data, which are accounted for in the analysis as a source of systematic uncertainty. These samples include ϕ mesons coming from pp interaction vertices and $B^0 \to J/\psi K^{*0}$ decays, with $J/\psi \to \mu^+\mu^-$. In the latter case, in order to emulate the signal behavior, the decay is reconstructed with the two muons not contributing to the vertex fitting. The resolution depends strongly on the decay time, with an average of 70 fs. The decay-time resolution is dominated by the photon momentum resolution, therefore being similar for $B_s^0 \to \phi\gamma$ and $B^0 \to K^{*0}\gamma$ decays.

The efficiency as a function of the decay time t is parametrized as

$$\epsilon(t) \propto \frac{t^{a/t}}{\cosh(bt)}, \tag{2}$$

where the parameters a and b describe mainly the shape of the function at low and high decay times, respectively. One hundred bins of variable size are defined to characterize this function. The efficiency parameters are determined in the simultaneous fit to the data, mainly driven from $B^0 \to K^{*0}\gamma$ candidates, while the differences between the two decays are obtained from the simulation and fixed in the data fit. In the simulation, the decay-time-dependent efficiencies of the two decay modes are compatible within uncertainties.

Pseudoexperiments are used to validate the overall fit procedure. In each pseudoexperiment, samples of $B_s^0 \to \phi\gamma$ and $B^0 \to K^{*0}\gamma$ signal decays are generated based on the data mass fit and the expected yields. Background candidates are included taking random events from the data or simulation. The mass and the decay-time fits are then performed, following the nominal procedure. The procedure is repeated for several values of the coefficients. No biases are found on the average fitted values, in any

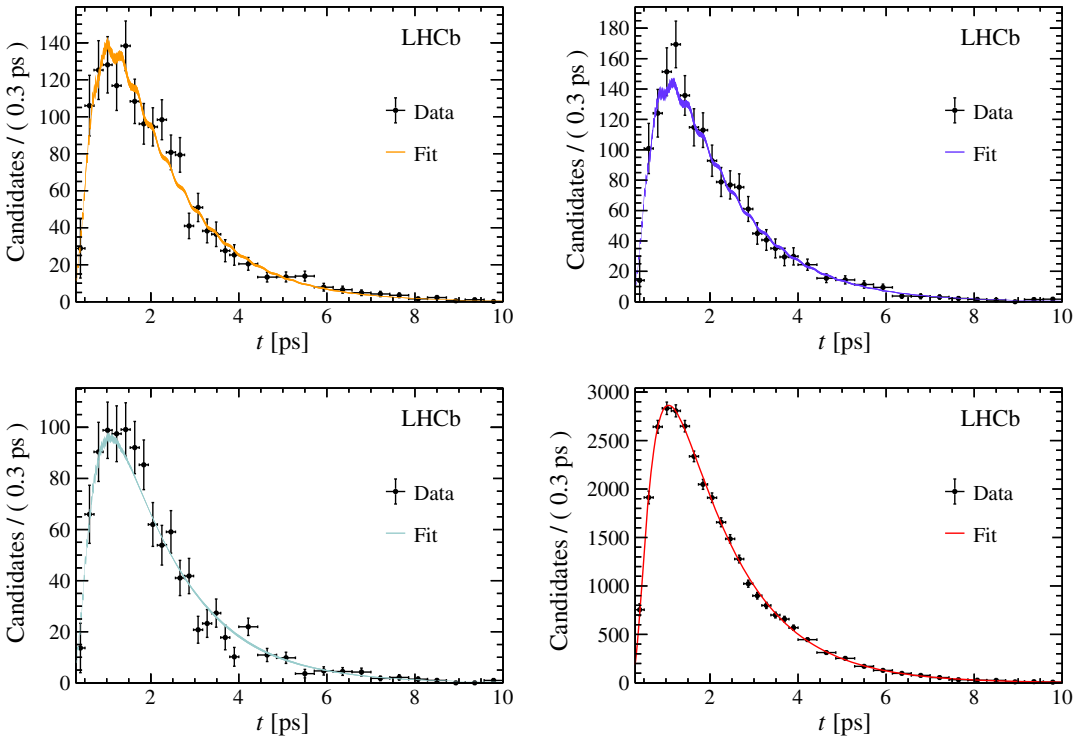

FIG. 2. Decay-time fit projections. The top row corresponds to the tagged (left) $B_s^0 \to \phi\gamma$ and (right) $\bar{B}_s^0 \to \phi\gamma$ candidates, while the bottom plots show the (left) untagged $B_s^0 \to \phi\gamma$ and (right) $B^0 \to K^{*0}\gamma$ candidates. The line is the result of the fit described in the text, including statistical uncertainties.

scenario. Statistical uncertainties are found to be underestimated by about 15% for $S_{\phi\gamma}$ and $C_{\phi\gamma}$ and 5% for $\mathcal{A}^{\Delta}_{\phi\gamma}$, due to the background-subtraction weights [26]. The uncertainties are corrected for in the results below.

The decay-time distributions and the corresponding fit projections are shown in Fig. 2. The fitted values are $S_{\phi\gamma} = 0.43 \pm 0.30$, $C_{\phi\gamma} = 0.11 \pm 0.29$, and $\mathcal{A}^{\Delta}_{\phi\gamma} = -0.67^{+0.37}_{-0.41}$, with a small correlation of -0.04 between each pair of observables. The statistical uncertainty includes the uncertainty from the physics parameters taken from external measurements. For $S_{\phi\gamma}$ and $C_{\phi\gamma}$, the systematic uncertainty is dominated by the effects of possible differences between the data and simulation in the decay-time resolution parameters (0.08) and the uncertainty on the parameters used to calibrate the same-side tagging algorithms (0.04). For $\mathcal{A}^{\Delta}_{\phi\gamma}$, the dominant source of systematic uncertainties is related to the determination of the decay-time-dependent efficiency function, in particular, the contribution of the partially reconstructed background of $B^0 \to K^{*0}\gamma$ decays, coming from the correlation between the reconstructed mass and time (0.11) and the mass-shape modeling (0.08), and the limited size of the simulation sample used to determine the efficiency differences between $B_s^0 \to \phi\gamma$ and $B^0 \to K^{*0}\gamma$ decays (0.08). The total systematic uncertainties are 0.11 for $S_{\phi\gamma}$ and $C_{\phi\gamma}$ and 0.17 for $\mathcal{A}^{\Delta}_{\phi\gamma}$.

In summary, the CP-violating and mixing-induced observables $S_{\phi\gamma}$, $C_{\phi\gamma}$, and $\mathcal{A}^{\Delta}_{\phi\gamma}$ are measured from a time-dependent analysis of $B_s^0 \to \phi\gamma$ decays, using a data sample corresponding to an integrated luminosity of 3 fb^{-1} collected with the LHCb experiment during the 2011 and 2012 data-taking periods. More than 5000 $B_s^0 \to \phi\gamma$ decays are reconstructed. A sample of $B^0 \to K^{*0}\gamma$ decays, which is 6 times larger, is used for the calibration of the time-dependent efficiency. From a simultaneous unbinned fit to the $B_s^0 \to \phi\gamma$ and $B^0 \to K^{*0}\gamma$ data samples, the values

$$S_{\phi\gamma} = 0.43 \pm 0.30 \pm 0.11,$$
$$C_{\phi\gamma} = 0.11 \pm 0.29 \pm 0.11,$$
$$\mathcal{A}^{\Delta}_{\phi\gamma} = -0.67^{+0.37}_{-0.41} \pm 0.17$$

are measured, where the first uncertainty is statistical and the second systematic. The results are compatible with the SM expectation [3] within 1.3, 0.3, and 1.7 standard deviations, respectively.

We express our gratitude to our colleagues in the CERN accelerator departments for the excellent performance of the LHC. We thank the technical and administrative staff at the LHCb institutes. We acknowledge support from CERN and from the national agencies: CAPES, CNPq, FAPERJ,

and FINEP (Brazil); MOST and NSFC (China); CNRS/IN2P3 (France); BMBF, DFG, and MPG (Germany); INFN (Italy); NWO (Netherlands); MNiSW and NCN (Poland); MEN/IFA (Romania); MSHE (Russia); MinECo (Spain); SNSF and SER (Switzerland); NASU (Ukraine); STFC (United Kingdom); DOE NP and NSF (USA). We acknowledge the computing resources that are provided by CERN, IN2P3 (France), KIT and DESY (Germany), INFN (Italy), SURF (Netherlands), PIC (Spain), GridPP (United Kingdom), RRCKI and Yandex LLC (Russia), CSCS (Switzerland), IFIN-HH (Romania), CBPF (Brazil), PL-GRID (Poland), and OSC (USA). We are indebted to the communities behind the multiple open-source software packages on which we depend. Individual groups or members have received support from AvH Foundation (Germany); EPLANET, Marie Skłodowska-Curie Actions, and ERC (European Union); ANR, Labex P2IO and OCEVU, and Région Auvergne-Rhône-Alpes (France); Key Research Program of Frontier Sciences of CAS, CAS PIFI, and the Thousand Talents Program (China); RFBR, RSF, and Yandex LLC (Russia); GVA, XuntaGal, and GENCAT (Spain); the Royal Society and the Leverhulme Trust (United Kingdom).

[1] D. Atwood, M. Gronau, and A. Soni, Mixing-Induced CP Asymmetries in Radiative B Decays in and Beyond the Standard Model, Phys. Rev. Lett. **79**, 185 (1997).

[2] D. Atwood, T. Gershon, M. Hazumi, and A. Soni, Mixing-induced CP violation in $B \to P_1 P_2 \gamma$ in search of clean new physics signals, Phys. Rev. D **71**, 076003 (2005).

[3] F. Muheim, Y. Xie, and R. Zwicky, Exploiting the width difference in $B_s \to \phi\gamma$, Phys. Lett. B **664**, 174 (2008).

[4] Y. Ushiroda *et al.* (Belle Collaboration), Time-dependent CP asymmetries in $B^0 \to K^0_S \pi^0 \gamma$ transitions, Phys. Rev. D **74**, 111104 (2006).

[5] B. Aubert *et al.* (*BABAR* Collaboration), Measurement of time-dependent CP asymmetry in $B^0 \to K^0_S \pi^0 \gamma$ decays, Phys. Rev. D **78**, 071102 (2008).

[6] R. Aaij *et al.* (LHCb Collaboration), Measurement of the ratio of branching fractions $\mathcal{B}(B^0 \to K^{*0}\gamma)/\mathcal{B}(B^0_s \to \phi\gamma)$ and the direct CP asymmetry in $B^0 \to K^{*0}\gamma$, Nucl. Phys. **B867**, 1 (2013).

[7] R. Aaij *et al.* (LHCb Collaboration), Angular analysis of the $B^0 \to K^{*0} e^+ e^-$ decay in the low-q^2 region, J. High Energy Phys. 04 (2015) 064.

[8] D. Dutta *et al.* (Belle Collaboration), Search for $B^0_s \to \gamma\gamma$ and a measurement of the branching fraction for $B^0_s \to \phi\gamma$, Phys. Rev. D **91**, 011101 (2015).

[9] R. Aaij *et al.* (LHCb Collaboration), First Experimental Study of Photon Polarization in Radiative B^0_s Decays, Phys. Rev. Lett. **118**, 021801 (2017).

[10] A. Paul and D. M. Straub, Constraints on new physics from radiative B decays, J. High Energy Phys. 04 (2017) 027.

[11] A. A. Alves Jr. *et al.* (LHCb Collaboration), The LHCb detector at the LHC, J. Instrum. **3**, S08005 (2008).

[12] R. Aaij *et al.* (LHCb Collaboration), LHCb detector performance, Int. J. Mod. Phys. A **30**, 1530022 (2015).

[13] T. Sjöstrand, S. Mrenna, and P. Skands, A brief introduction to PYTHIA 8.1, Comput. Phys. Commun. **178**, 852 (2008); PYTHIA 6.4 physics and manual, J. High Energy Phys. 05 (2006) 026.

[14] I. Belyaev *et al.*, Handling of the generation of primary events in Gauss, the LHCb simulation framework, J. Phys. Conf. Ser. **331**, 032047 (2011).

[15] D. J. Lange, The EvtGen particle decay simulation package, Nucl. Instrum. Methods Phys. Res., Sect. A **462**, 152 (2001).

[16] P. Golonka and Z. Was, PHOTOS Monte Carlo: A precision tool for QED corrections in Z and W decays, Eur. Phys. J. C **45**, 97 (2006).

[17] J. Allison *et al.* (Geant4 Collaboration), Geant4 developments and applications, IEEE Trans. Nucl. Sci. **53**, 270 (2006); S. Agostinelli *et al.* (Geant4 Collaboration), Geant4: A simulation toolkit, Nucl. Instrum. Methods Phys. Res., Sect. A **506**, 250 (2003).

[18] M. Clemencic, G Corti, S Easo, C R Jones, S Miglioranzi, M Pappagallo, and P Robbe, The LHCb simulation application, Gauss: Design, evolution and experience, J. Phys. Conf. Ser. **331**, 032023 (2011).

[19] M. Calvo Gomez *et al.*, A tool for γ/π^0 separation at high energies, CERN Report No. LHCb-PUB-2015-016, 2015.

[20] M. Tanabashi *et al.* (Particle Data Group), Review of particle physics, Phys. Rev. D **98**, 030001 (2018).

[21] M. Pivk and F. R. Le Diberder, sPlot: A statistical tool to unfold data distributions, Nucl. Instrum. Methods Phys. Res., Sect. A **555**, 356 (2005).

[22] T. Skwarnicki, A study of the radiative cascade transitions between the Upsilon-prime and Upsilon resonances, Ph.D. thesis, Institute of Nuclear Physics, 1986, DESY-F31-86-02.

[23] H. Albrecht *et al.* (ARGUS Collaboration), Search for hadronic $b \to u$ decays, Phys. Lett. B **241**, 278 (1990).

[24] R. Aaij *et al.* (LHCb Collaboration), A new algorithm for identifying the flavour of B^0_s mesons at LHCb, J. Instrum. **11**, P05010 (2016).

[25] R. Aaij *et al.* (LHCb Collaboration), Opposite-side flavour tagging of B mesons at the LHCb experiment, Eur. Phys. J. C **72**, 2022 (2012).

[26] Y. Xie, sFit: A method for background subtraction in maximum likelihood fit, arXiv:0905.0724.

[27] Y. Amhis *et al.* (Heavy Flavor Averaging Group), Averages of b-hadron, c-hadron, and τ-lepton properties as of summer 2016, Eur. Phys. J. C **77**, 895 (2017), updated results and plots available at https://hflav.web.cern.ch.

R. Aaij,[29] C. Abellán Beteta,[46] B. Adeva,[43] M. Adinolfi,[50] C. A. Aidala,[77] Z. Ajaltouni,[7] S. Akar,[61] P. Albicocco,[20] J. Albrecht,[12] F. Alessio,[44] M. Alexander,[55] A. Alfonso Albero,[42] G. Alkhazov,[35] P. Alvarez Cartelle,[57] A. A. Alves Jr.,[43] S. Amato,[2] Y. Amhis,[9] L. An,[19] L. Anderlini,[19] G. Andreassi,[45] M. Andreotti,[18] J. E. Andrews,[62] F. Archilli,[20] J. Arnau Romeu,[8] A. Artamonov,[41] M. Artuso,[63] K. Arzymatov,[39] E. Aslanides,[8] M. Atzeni,[46] B. Audurier,[24] S. Bachmann,[14] J. J. Back,[52] S. Baker,[57] V. Balagura,[9,b] W. Baldini,[18,44] A. Baranov,[39] R. J. Barlow,[58] S. Barsuk,[9] W. Barter,[57] M. Bartolini,[21] F. Baryshnikov,[73] V. Batozskaya,[33] B. Batsukh,[63] A. Battig,[12] V. Battista,[45] A. Bay,[45] F. Bedeschi,[26] I. Bediaga,[1] A. Beiter,[63] L. J. Bel,[29] V. Belavin,[39] S. Belin,[24] N. Beliy,[4] V. Bellee,[45] N. Belloli,[22,c] K. Belous,[41] I. Belyaev,[36] G. Bencivenni,[20] E. Ben-Haim,[10] S. Benson,[29] S. Beranek,[11] A. Berezhnoy,[37] R. Bernet,[46] D. Berninghoff,[14] E. Bertholet,[10] A. Bertolin,[25] C. Betancourt,[46] F. Betti,[17,d] M. O. Bettler,[51] Ia. Bezshyiko,[46] S. Bhasin,[50] J. Bhom,[31] M. S. Bieker,[12] S. Bifani,[49] P. Billoir,[10] A. Birnkraut,[12] A. Bizzeti,[19,e] M. Bjørn,[59] M. P. Blago,[44] T. Blake,[52] F. Blanc,[45] S. Blusk,[63] D. Bobulska,[55] V. Bocci,[28] O. Boente Garcia,[43] T. Boettcher,[60] A. Bondar,[40,f] N. Bondar,[35] S. Borghi,[58,44] M. Borisyak,[39] M. Borsato,[14] M. Boubdir,[11] T. J. V. Bowcock,[56] C. Bozzi,[18,44] S. Braun,[14] A. Brea Rodriguez,[43] M. Brodski,[44] J. Brodzicka,[31] A. Brossa Gonzalo,[52] D. Brundu,[24,44] E. Buchanan,[50] A. Buonaura,[46] C. Burr,[58] A. Bursche,[24] J. S. Butter,[29] J. Buytaert,[44] W. Byczynski,[44] S. Cadeddu,[24] H. Cai,[67] R. Calabrese,[18,g] S. Cali,[20] R. Calladine,[49] M. Calvi,[22,c] M. Calvo Gomez,[42,h] A. Camboni,[42,h] P. Campana,[20] D. H. Campora Perez,[44] L. Capriotti,[17,d] A. Carbone,[17,d] G. Carboni,[27] R. Cardinale,[21] A. Cardini,[24] P. Carniti,[22,c] K. Carvalho Akiba,[2] A. Casais Vidal,[43] G. Casse,[56] M. Cattaneo,[44] G. Cavallero,[21] R. Cenci,[26,i] M. G. Chapman,[50] M. Charles,[10,44] Ph. Charpentier,[44] G. Chatzikonstantinidis,[49] M. Chefdeville,[6] V. Chekalina,[39] C. Chen,[3] S. Chen,[24] S.-G. Chitic,[44] V. Chobanova,[43] M. Chrzaszcz,[44] A. Chubykin,[35] P. Ciambrone,[20] X. Cid Vidal,[43] G. Ciezarek,[44] F. Cindolo,[17] P. E. L. Clarke,[54] M. Clemencic,[44] H. V. Cliff,[51] J. Closier,[44] V. Coco,[44] J. A. B. Coelho,[9] J. Cogan,[8] E. Cogneras,[7] L. Cojocariu,[34] P. Collins,[44] T. Colombo,[44] A. Comerma-Montells,[14] A. Contu,[24] G. Coombs,[44] S. Coquereau,[42] G. Corti,[44] C. M. Costa Sobral,[52] B. Couturier,[44] G. A. Cowan,[54] D. C. Craik,[60] A. Crocombe,[52] M. Cruz Torres,[1] R. Currie,[54] C. L. Da Silva,[78] E. Dall'Occo,[29] J. Dalseno,[43,j] C. D'Ambrosio,[44] A. Danilina,[36] P. d'Argent,[14] A. Davis,[58] O. De Aguiar Francisco,[44] K. De Bruyn,[44] S. De Capua,[58] M. De Cian,[45] J. M. De Miranda,[1] L. De Paula,[2] M. De Serio,[16,k] P. De Simone,[20] J. A. de Vries,[29] C. T. Dean,[55] W. Dean,[77] D. Decamp,[6] L. Del Buono,[10] B. Delaney,[51] H.-P. Dembinski,[13] M. Demmer,[12] A. Dendek,[32] D. Derkach,[74] O. Deschamps,[7] F. Desse,[9] F. Dettori,[24] B. Dey,[68] A. Di Canto,[44] P. Di Nezza,[20] S. Didenko,[73] H. Dijkstra,[44] F. Dordei,[24] M. Dorigo,[26,l] A. C. dos Reis,[1] A. Dosil Suárez,[43] L. Douglas,[55] A. Dovbnya,[47] K. Dreimanis,[56] L. Dufour,[44] G. Dujany,[10] P. Durante,[44] J. M. Durham,[78] D. Dutta,[58] R. Dzhelyadin,[41,a] M. Dziewiecki,[14] A. Dziurda,[31] A. Dzyuba,[35] S. Easo,[53] U. Egede,[57] V. Egorychev,[36] S. Eidelman,[40,f] S. Eisenhardt,[54] U. Eitschberger,[12] R. Ekelhof,[12] S. Ek-In,[45] L. Eklund,[55] S. Ely,[63] A. Ene,[34] S. Escher,[11] S. Esen,[29] T. Evans,[61] A. Falabella,[17] C. Färber,[44] N. Farley,[49] S. Farry,[56] D. Fazzini,[9] M. Féo,[44] P. Fernandez Declara,[44] A. Fernandez Prieto,[43] F. Ferrari,[17,d] L. Ferreira Lopes,[45] F. Ferreira Rodrigues,[2] S. Ferreres Sole,[29] M. Ferro-Luzzi,[44] S. Filippov,[38] R. A. Fini,[16] M. Fiorini,[18,g] M. Firlej,[32] C. Fitzpatrick,[44] T. Fiutowski,[32] F. Fleuret,[9,b] M. Fontana,[44] F. Fontanelli,[21,m] R. Forty,[44] V. Franco Lima,[56] M. Franco Sevilla,[62] M. Frank,[44] C. Frei,[44] J. Fu,[23,n] W. Funk,[44] E. Gabriel,[54] A. Gallas Torreira,[43] D. Galli,[17,d] S. Gallorini,[25] S. Gambetta,[54] Y. Gan,[3] M. Gandelman,[2] P. Gandini,[23] Y. Gao,[3] L. M. Garcia Martin,[76] J. García Pardiñas,[46] B. Garcia Plana,[43] J. Garra Tico,[51] L. Garrido,[42] D. Gascon,[42] C. Gaspar,[44] G. Gazzoni,[7] D. Gerick,[14] E. Gersabeck,[58] M. Gersabeck,[58] T. Gershon,[52] D. Gerstel,[8] Ph. Ghez,[6] V. Gibson,[51] O. G. Girard,[45] P. Gironella Gironell,[42] L. Giubega,[34] K. Gizdov,[54] V. V. Gligorov,[10] C. Göbel,[65] D. Golubkov,[36] A. Golutvin,[57,73] A. Gomes,[1,o] I. V. Gorelov,[37] C. Gotti,[22,c] E. Govorkova,[29] J. P. Grabowski,[14] R. Graciani Diaz,[42] L. A. Granado Cardoso,[44] E. Graugés,[42] E. Graverini,[45] G. Graziani,[19] A. Grecu,[34] R. Greim,[29] P. Griffith,[24] L. Grillo,[58] L. Gruber,[44] B. R. Gruberg Cazon,[59] C. Gu,[3] E. Gushchin,[38] A. Guth,[11] Yu. Guz,[41,44] T. Gys,[44] T. Hadavizadeh,[59] C. Hadjivasiliou,[7] G. Haefeli,[45] C. Haen,[44] S. C. Haines,[51] B. Hamilton,[62] Q. Han,[68] X. Han,[14] T. H. Hancock,[59] S. Hansmann-Menzemer,[14] N. Harnew,[59] T. Harrison,[56] C. Hasse,[44] M. Hatch,[44] J. He,[4] M. Hecker,[57] K. Heinicke,[12] A. Heister,[12] K. Hennessy,[56] L. Henry,[76] M. Heß,[70] J. Heuel,[11] A. Hicheur,[64] R. Hidalgo Charman,[58] D. Hill,[59] M. Hilton,[58] P. H. Hopchev,[45] J. Hu,[14] W. Hu,[68] W. Huang,[4] Z. C. Huard,[61] W. Hulsbergen,[29] T. Humair,[57] M. Hushchyn,[74] D. Hutchcroft,[56] D. Hynds,[29] P. Ibis,[12] M. Idzik,[32] P. Ilten,[49] A. Inglessi,[35] A. Inyakin,[41] K. Ivshin,[35] R. Jacobsson,[44] S. Jakobsen,[44] J. Jalocha,[59] E. Jans,[29] B. K. Jashal,[76] A. Jawahery,[62] F. Jiang,[3] M. John,[59] D. Johnson,[44] C. R. Jones,[51] C. Joram,[44] B. Jost,[44] N. Jurik,[59] S. Kandybei,[47] M. Karacson,[44] J. M. Kariuki,[50] S. Karodia,[55] N. Kazeev,[74] M. Kecke,[14] F. Keizer,[51] M. Kelsey,[63] M. Kenzie,[51] T. Ketel,[30] B. Khanji,[44] A. Kharisova,[75] C. Khurewathanakul,[45] K. E. Kim,[63] T. Kirn,[11] V. S. Kirsebom,[45] S. Klaver,[20] K. Klimaszewski,[33] S. Koliiev,[48] M. Kolpin,[14] A. Kondybayeva,[73]

A. Konoplyannikov,[36] R. Kopecna,[14] P. Koppenburg,[29] I. Kostiuk,[29,48] O. Kot,[48] S. Kotriakhova,[35] M. Kozeiha,[7] L. Kravchuk,[38] M. Kreps,[52] F. Kress,[57] S. Kretzschmar,[11] P. Krokovny,[40,f] W. Krupa,[32] W. Krzemien,[33] W. Kucewicz,[31,p] M. Kucharczyk,[31] V. Kudryavtsev,[40,f] G. J. Kunde,[78] A. K. Kuonen,[45] T. Kvaratskheliya,[36] D. Lacarrere,[44] G. Lafferty,[58] A. Lai,[24] D. Lancierini,[46] G. Lanfranchi,[20] C. Langenbruch,[11] T. Latham,[52] C. Lazzeroni,[49] R. Le Gac,[8] R. Lefèvre,[7] A. Leflat,[37] F. Lemaitre,[44] O. Leroy,[8] T. Lesiak,[31] B. Leverington,[14] H. Li,[66] P.-R. Li,[4,q] X. Li,[78] Y. Li,[5] Z. Li,[63] X. Liang,[63] T. Likhomanenko,[72] R. Lindner,[44] F. Lionetto,[46] V. Lisovskyi,[9] G. Liu,[66] X. Liu,[3] D. Loh,[52] A. Loi,[24] J. Lomba Castro,[43] I. Longstaff,[55] J. H. Lopes,[2] G. Loustau,[46] G. H. Lovell,[51] D. Lucchesi,[25,r] M. Lucio Martinez,[43] Y. Luo,[3] A. Lupato,[25] E. Luppi,[18,g] O. Lupton,[52] A. Lusiani,[26] X. Lyu,[4] F. Machefert,[9] F. Maciuc,[34] V. Macko,[45] P. Mackowiak,[12] S. Maddrell-Mander,[50] O. Maev,[35,44] K. Maguire,[58] D. Maisuzenko,[35] M. W. Majewski,[32] S. Malde,[59] B. Malecki,[44] A. Malinin,[72] T. Maltsev,[40,f] H. Malygina,[14] G. Manca,[24,s] G. Mancinelli,[8] D. Marangotto,[23,n] J. Maratas,[7,t] J. F. Marchand,[6] U. Marconi,[17] C. Marin Benito,[9] M. Marinangeli,[45] P. Marino,[45] J. Marks,[14] P. J. Marshall,[56] G. Martellotti,[28] L. Martinazzoli,[44] M. Martinelli,[44,22,c] D. Martinez Santos,[43] F. Martinez Vidal,[76] A. Massafferri,[1] M. Materok,[11] R. Matev,[44] A. Mathad,[46] Z. Mathe,[44] V. Matiunin,[36] C. Matteuzzi,[22] K. R. Mattioli,[77] A. Mauri,[46] E. Maurice,[9,b] B. Maurin,[45] M. McCann,[57,44] A. McNab,[58] R. McNulty,[15] J. V. Mead,[56] B. Meadows,[61] C. Meaux,[8] N. Meinert,[70] D. Melnychuk,[33] M. Merk,[29] A. Merli,[23,n] E. Michielin,[25] D. A. Milanes,[69] E. Millard,[52] M.-N. Minard,[6] O. Mineev,[36] L. Minzoni,[18,g] D. S. Mitzel,[14] A. Mödden,[12] A. Mogini,[10] R. D. Moise,[57] T. Mombächer,[12] I. A. Monroy,[69] S. Monteil,[7] M. Morandin,[25] G. Morello,[20] M. J. Morello,[26,u] J. Moron,[32] A. B. Morris,[8] R. Mountain,[63] H. Mu,[3] F. Muheim,[54] M. Mukherjee,[68] M. Mulder,[29] D. Müller,[44] J. Müller,[12] K. Müller,[46] V. Müller,[12] C. H. Murphy,[59] D. Murray,[58] P. Naik,[50] T. Nakada,[45] R. Nandakumar,[53] A. Nandi,[59] T. Nanut,[45] I. Nasteva,[2] M. Needham,[54] N. Neri,[23,n] S. Neubert,[14] N. Neufeld,[44] R. Newcombe,[57] T. D. Nguyen,[45] C. Nguyen-Mau,[45,v] S. Nieswand,[11] R. Niet,[12] N. Nikitin,[37] N. S. Nolte,[44] A. Oblakowska-Mucha,[32] V. Obraztsov,[41] S. Ogilvy,[55] D. P. O'Hanlon,[17] R. Oldeman,[24,s] C. J. G. Onderwater,[71] J. D. Osborn,[77] A. Ossowska,[31] J. M. Otalora Goicochea,[2] T. Ovsiannikova,[36] P. Owen,[46] A. Oyanguren,[76] P. R. Pais,[45] T. Pajero,[26,u] A. Palano,[16] M. Palutan,[20] G. Panshin,[75] A. Papanestis,[53] M. Pappagallo,[54] L. L. Pappalardo,[18,g] W. Parker,[62] C. Parkes,[58,44] G. Passaleva,[19,44] A. Pastore,[16] M. Patel,[57] C. Patrignani,[17,d] A. Pearce,[44] A. Pellegrino,[29] G. Penso,[28] M. Pepe Altarelli,[44] S. Perazzini,[17] D. Pereima,[36] P. Perret,[7] L. Pescatore,[45] K. Petridis,[50] A. Petrolini,[21,m] A. Petrov,[72] S. Petrucci,[54] M. Petruzzo,[23,n] B. Pietrzyk,[6] G. Pietrzyk,[45] M. Pikies,[31] M. Pili,[59] D. Pinci,[28] J. Pinzino,[44] F. Pisani,[44] A. Piucci,[14] V. Placinta,[34] S. Playfer,[54] J. Plews,[49] M. Plo Casasus,[43] F. Polci,[10] M. Poli Lener,[20] M. Poliakova,[63] A. Poluektov,[8] N. Polukhina,[73,w] I. Polyakov,[63] E. Polycarpo,[2] G. J. Pomery,[50] S. Ponce,[44] A. Popov,[41] D. Popov,[49] S. Poslavskii,[41] E. Price,[50] C. Prouve,[43] V. Pugatch,[48] A. Puig Navarro,[46] H. Pullen,[59] G. Punzi,[26,i] W. Qian,[4] J. Qin,[4] R. Quagliani,[10] B. Quintana,[7] N. V. Raab,[15] B. Rachwal,[32] J. H. Rademacker,[50] M. Rama,[26] M. Ramos Pernas,[43] M. S. Rangel,[2] F. Ratnikov,[39,74] G. Raven,[30] M. Ravonel Salzgeber,[44] M. Reboud,[6] F. Redi,[45] S. Reichert,[12] F. Reiss,[10] C. Remon Alepuz,[76] Z. Ren,[3] V. Renaudin,[59] S. Ricciardi,[53] S. Richards,[50] K. Rinnert,[56] P. Robbe,[9] A. Robert,[10] A. B. Rodrigues,[45] E. Rodrigues,[61] J. A. Rodriguez Lopez,[69] M. Roehrken,[44] S. Roiser,[44] A. Rollings,[59] V. Romanovskiy,[41] A. Romero Vidal,[43] J. D. Roth,[77] M. Rotondo,[20] M. S. Rudolph,[63] T. Ruf,[44] J. Ruiz Vidal,[76] J. J. Saborido Silva,[43] N. Sagidova,[35] B. Saitta,[24,s] V. Salustino Guimaraes,[65] C. Sanchez Gras,[29] C. Sanchez Mayordomo,[76] B. Sanmartin Sedes,[43] R. Santacesaria,[28] C. Santamarina Rios,[43] M. Santimaria,[20,44] E. Santovetti,[27,x] G. Sarpis,[58] A. Sarti,[20,y] C. Satriano,[28,z] A. Satta,[27] M. Saur,[4] D. Savrina,[36,37] S. Schael,[11] M. Schellenberg,[12] M. Schiller,[55] H. Schindler,[44] M. Schmelling,[13] T. Schmelzer,[12] B. Schmidt,[44] O. Schneider,[45] A. Schopper,[44] H. F. Schreiner,[61] M. Schubiger,[29] S. Schulte,[45] M. H. Schune,[9] R. Schwemmer,[44] B. Sciascia,[20] A. Sciubba,[28,y] A. Semennikov,[36] E. S. Sepulveda,[10] A. Sergi,[49,44] N. Serra,[46] J. Serrano,[8] L. Sestini,[25] A. Seuthe,[12] P. Seyfert,[44] M. Shapkin,[41] T. Shears,[56] L. Shekhtman,[40,f] V. Shevchenko,[72] E. Shmanin,[73] B. G. Siddi,[18] R. Silva Coutinho,[46] L. Silva de Oliveira,[2] G. Simi,[25,r] S. Simone,[16,k] I. Skiba,[18] N. Skidmore,[14] T. Skwarnicki,[63] M. W. Slater,[49] J. G. Smeaton,[51] E. Smith,[11] I. T. Smith,[54] M. Smith,[57] M. Soares,[17] l. Soares Lavra,[1] M. D. Sokoloff,[61] F. J. P. Soler,[55] B. Souza De Paula,[2] B. Spaan,[12] E. Spadaro Norella,[23,n] P. Spradlin,[55] F. Stagni,[44] M. Stahl,[14] S. Stahl,[44] P. Stefko,[45] S. Stefkova,[57] O. Steinkamp,[46] S. Stemmle,[14] O. Stenyakin,[41] M. Stepanova,[35] H. Stevens,[12] A. Stocchi,[9] S. Stone,[63] S. Stracka,[26] M. E. Stramaglia,[45] M. Straticiuc,[34] U. Straumann,[46] S. Strokov,[75] J. Sun,[3] L. Sun,[67] Y. Sun,[62] K. Swientek,[32] A. Szabelski,[33] T. Szumlak,[32] M. Szymanski,[4] Z. Tang,[3] T. Tekampe,[12] G. Tellarini,[18] F. Teubert,[44] E. Thomas,[44] M. J. Tilley,[57] V. Tisserand,[7] S. T'Jampens,[6] M. Tobin,[5] S. Tolk,[44] L. Tomassetti,[18,g] D. Tonelli,[26] D. Y. Tou,[10] E. Tournefier,[6] M. Traill,[55] M. T. Tran,[45] A. Trisovic,[51] A. Tsaregorodtsev,[8] G. Tuci,[26,44,i] A. Tully,[51] N. Tuning,[29] A. Ukleja,[33] A. Usachov,[9] A. Ustyuzhanin,[39,74] U. Uwer,[14] A. Vagner,[75] V. Vagnoni,[17]

A. Valassi,[44] S. Valat,[44] G. Valenti,[17] M. van Beuzekom,[29] H. Van Hecke,[78] E. van Herwijnen,[44] C. B. Van Hulse,[15] J. van Tilburg,[29] M. van Veghel,[29] R. Vazquez Gomez,[44] P. Vazquez Regueiro,[43] C. Vázquez Sierra,[29] S. Vecchi,[18] J. J. Velthuis,[50] M. Veltri,[19,aa] A. Venkateswaran,[63] M. Vernet,[7] M. Veronesi,[29] M. Vesterinen,[52] J. V. Viana Barbosa,[44] D. Vieira,[4] M. Vieites Diaz,[43] H. Viemann,[70] X. Vilasis-Cardona,[42,h] A. Vitkovskiy,[29] M. Vitti,[51] V. Volkov,[37] A. Vollhardt,[46] D. Vom Bruch,[10] B. Voneki,[44] A. Vorobyev,[35] V. Vorobyev,[40,f] N. Voropaev,[35] R. Waldi,[70] J. Walsh,[26] J. Wang,[3] J. Wang,[5] M. Wang,[3] Y. Wang,[68] Z. Wang,[46] D. R. Ward,[51] H. M. Wark,[56] N. K. Watson,[49] D. Websdale,[57] A. Weiden,[46] C. Weisser,[60] M. Whitehead,[11] G. Wilkinson,[59] M. Wilkinson,[63] I. Williams,[51] M. Williams,[60] M. R. J. Williams,[58] T. Williams,[49] F. F. Wilson,[53] M. Winn,[9] W. Wislicki,[33] M. Witek,[31] G. Wormser,[9] S. A. Wotton,[51] K. Wyllie,[44] D. Xiao,[68] Y. Xie,[68] H. Xing,[66] A. Xu,[3] L. Xu,[3] M. Xu,[68] Q. Xu,[4] Z. Xu,[6] Z. Xu,[3] Z. Yang,[3] Z. Yang,[62] Y. Yao,[63] L. E. Yeomans,[56] H. Yin,[68] J. Yu,[68,bb] X. Yuan,[63] O. Yushchenko,[41] K. A. Zarebski,[49] M. Zavertyaev,[13,w] M. Zeng,[3] D. Zhang,[68] L. Zhang,[3] S. Zhang,[3] W. C. Zhang,[3,cc] Y. Zhang,[44] A. Zhelezov,[14] Y. Zheng,[4] X. Zhu,[3] V. Zhukov,[11,37] J. B. Zonneveld,[54] and S. Zucchelli[17,d]

(LHCb Collaboration)

[1]*Centro Brasileiro de Pesquisas Físicas (CBPF), Rio de Janeiro, Brazil*
[2]*Universidade Federal do Rio de Janeiro (UFRJ), Rio de Janeiro, Brazil*
[3]*Center for High Energy Physics, Tsinghua University, Beijing, China*
[4]*University of Chinese Academy of Sciences, Beijing, China*
[5]*Institute Of High Energy Physics (ihep), Beijing, China*
[6]*Univ. Grenoble Alpes, Univ. Savoie Mont Blanc, CNRS, IN2P3-LAPP, Annecy, France*
[7]*Université Clermont Auvergne, CNRS/IN2P3, LPC, Clermont-Ferrand, France*
[8]*Aix Marseille Univ, CNRS/IN2P3, CPPM, Marseille, France*
[9]*LAL, Univ. Paris-Sud, CNRS/IN2P3, Université Paris-Saclay, Orsay, France*
[10]*LPNHE, Sorbonne Université, Paris Diderot Sorbonne Paris Cité, CNRS/IN2P3, Paris, France*
[11]*I. Physikalisches Institut, RWTH Aachen University, Aachen, Germany*
[12]*Fakultät Physik, Technische Universität Dortmund, Dortmund, Germany*
[13]*Max-Planck-Institut für Kernphysik (MPIK), Heidelberg, Germany*
[14]*Physikalisches Institut, Ruprecht-Karls-Universität Heidelberg, Heidelberg, Germany*
[15]*School of Physics, University College Dublin, Dublin, Ireland*
[16]*INFN Sezione di Bari, Bari, Italy*
[17]*INFN Sezione di Bologna, Bologna, Italy*
[18]*INFN Sezione di Ferrara, Ferrara, Italy*
[19]*INFN Sezione di Firenze, Firenze, Italy*
[20]*INFN Laboratori Nazionali di Frascati, Frascati, Italy*
[21]*INFN Sezione di Genova, Genova, Italy*
[22]*INFN Sezione di Milano-Bicocca, Milano, Italy*
[23]*INFN Sezione di Milano, Milano, Italy*
[24]*INFN Sezione di Cagliari, Monserrato, Italy*
[25]*INFN Sezione di Padova, Padova, Italy*
[26]*INFN Sezione di Pisa, Pisa, Italy*
[27]*INFN Sezione di Roma Tor Vergata, Roma, Italy*
[28]*INFN Sezione di Roma La Sapienza, Roma, Italy*
[29]*Nikhef National Institute for Subatomic Physics, Amsterdam, Netherlands*
[30]*Nikhef National Institute for Subatomic Physics and VU University Amsterdam, Amsterdam, Netherlands*
[31]*Henryk Niewodniczanski Institute of Nuclear Physics Polish Academy of Sciences, Kraków, Poland*
[32]*AGH—University of Science and Technology, Faculty of Physics and Applied Computer Science, Kraków, Poland*
[33]*National Center for Nuclear Research (NCBJ), Warsaw, Poland*
[34]*Horia Hulubei National Institute of Physics and Nuclear Engineering, Bucharest-Magurele, Romania*
[35]*Petersburg Nuclear Physics Institute NRC Kurchatov Institute (PNPI NRC KI), Gatchina, Russia*
[36]*Institute of Theoretical and Experimental Physics NRC Kurchatov Institute (ITEP NRC KI), Moscow, Russia, Moscow, Russia*
[37]*Institute of Nuclear Physics, Moscow State University (SINP MSU), Moscow, Russia*
[38]*Institute for Nuclear Research of the Russian Academy of Sciences (INR RAS), Moscow, Russia*
[39]*Yandex School of Data Analysis, Moscow, Russia*
[40]*Budker Institute of Nuclear Physics (SB RAS), Novosibirsk, Russia*
[41]*Institute for High Energy Physics NRC Kurchatov Institute (IHEP NRC KI), Protvino, Russia, Protvino, Russia*
[42]*ICCUB, Universitat de Barcelona, Barcelona, Spain*

[43]Instituto Galego de Física de Altas Enerxías (IGFAE), Universidade de Santiago de Compostela, Santiago de Compostela, Spain
[44]European Organization for Nuclear Research (CERN), Geneva, Switzerland
[45]Institute of Physics, Ecole Polytechnique Fédérale de Lausanne (EPFL), Lausanne, Switzerland
[46]Physik-Institut, Universität Zürich, Zürich, Switzerland
[47]NSC Kharkiv Institute of Physics and Technology (NSC KIPT), Kharkiv, Ukraine
[48]Institute for Nuclear Research of the National Academy of Sciences (KINR), Kyiv, Ukraine
[49]University of Birmingham, Birmingham, United Kingdom
[50]H.H. Wills Physics Laboratory, University of Bristol, Bristol, United Kingdom
[51]Cavendish Laboratory, University of Cambridge, Cambridge, United Kingdom
[52]Department of Physics, University of Warwick, Coventry, United Kingdom
[53]STFC Rutherford Appleton Laboratory, Didcot, United Kingdom
[54]School of Physics and Astronomy, University of Edinburgh, Edinburgh, United Kingdom
[55]School of Physics and Astronomy, University of Glasgow, Glasgow, United Kingdom
[56]Oliver Lodge Laboratory, University of Liverpool, Liverpool, United Kingdom
[57]Imperial College London, London, United Kingdom
[58]School of Physics and Astronomy, University of Manchester, Manchester, United Kingdom
[59]Department of Physics, University of Oxford, Oxford, United Kingdom
[60]Massachusetts Institute of Technology, Cambridge, Massachusetts, USA
[61]University of Cincinnati, Cincinnati, Ohio, USA
[62]University of Maryland, College Park, Maryland, USA
[63]Syracuse University, Syracuse, New York, USA
[64]Laboratory of Mathematical and Subatomic Physics, Constantine, Algeria
[associated with Universidade Federal do Rio de Janeiro (UFRJ), Rio de Janeiro, Brazil]
[65]Pontifícia Universidade Católica do Rio de Janeiro (PUC-Rio), Rio de Janeiro, Brazil
[associated with Universidade Federal do Rio de Janeiro (UFRJ), Rio de Janeiro, Brazil]
[66]South China Normal University, Guangzhou, China
(associated with Center for High Energy Physics, Tsinghua University, Beijing, China)
[67]School of Physics and Technology, Wuhan University, Wuhan, China
(associated with Center for High Energy Physics, Tsinghua University, Beijing, China)
[68]Institute of Particle Physics, Central China Normal University, Wuhan, Hubei, China
(associated with Center for High Energy Physics, Tsinghua University, Beijing, China)
[69]Departamento de Fisica, Universidad Nacional de Colombia, Bogota, Colombia
(associated with LPNHE, Sorbonne Université, Paris Diderot Sorbonne Paris Cité, CNRS/IN2P3, Paris, France)
[70]Institut für Physik, Universität Rostock, Rostock, Germany
(associated with Physikalisches Institut, Ruprecht-Karls-Universität Heidelberg, Heidelberg, Germany)
[71]Van Swinderen Institute, University of Groningen, Groningen, Netherlands
(associated with Nikhef National Institute for Subatomic Physics, Amsterdam, Netherlands)
[72]National Research Centre Kurchatov Institute, Moscow, Russia
[associated with Institute of Theoretical and Experimental Physics NRC Kurchatov Institute (ITEP NRC KI), Moscow, Russia, Moscow, Russia]
[73]National University of Science and Technology "MISIS", Moscow, Russia
[associated with Institute of Theoretical and Experimental Physics NRC Kurchatov Institute (ITEP NRC KI), Moscow, Russia, Moscow, Russia]
[74]National Research University Higher School of Economics, Moscow, Russia
[associated with Yandex School of Data Analysis, Moscow, Russia]
[75]National Research Tomsk Polytechnic University, Tomsk, Russia
[associated with Institute of Theoretical and Experimental Physics NRC Kurchatov Institute (ITEP NRC KI), Moscow, Russia, Moscow, Russia]
[76]Instituto de Fisica Corpuscular, Centro Mixto Universidad de Valencia—CSIC, Valencia, Spain
(associated with ICCUB, Universitat de Barcelona, Barcelona, Spain)
[77]University of Michigan, Ann Arbor, USA
(associated with Syracuse University, Syracuse, New York, USA)
[78]Los Alamos National Laboratory (LANL), Los Alamos, USA
(associated with Syracuse University, Syracuse, New York, USA)

[a]Deceased.
[b]Also at Laboratoire Leprince-Ringuet, Palaiseau, France.
[c]Also at Università di Milano Bicocca, Milano, Italy.
[d]Also at Università di Bologna, Bologna, Italy.
[e]Also at Università di Modena e Reggio Emilia, Modena, Italy.

[f]Also at Novosibirsk State University, Novosibirsk, Russia.
[g]Also at Università di Ferrara, Ferrara, Italy.
[h]Also at LIFAELS, La Salle, Universitat Ramon Llull, Barcelona, Spain.
[i]Also at Università di Pisa, Pisa, Italy.
[j]Also at H.H. Wills Physics Laboratory, University of Bristol, Bristol, United Kingdom.
[k]Also at Università di Bari, Bari, Italy.
[l]Also at Sezione INFN di Trieste, Trieste, Italy.
[m]Also at Università di Genova, Genova, Italy.
[n]Also at Università degli Studi di Milano, Milano, Italy.
[o]Also at Universidade Federal do Triângulo Mineiro (UFTM), Uberaba-MG, Brazil.
[p]Also at AGH—University of Science and Technology, Faculty of Computer Science, Electronics and Telecommunications, Kraków, Poland.
[q]Also at Lanzhou University, Lanzhou, China.
[r]Also at Università di Padova, Padova, Italy.
[s]Also at Università di Cagliari, Cagliari, Italy.
[t]Also at MSU—Iligan Institute of Technology (MSU-IIT), Iligan, Philippines.
[u]Also at Scuola Normale Superiore, Pisa, Italy.
[v]Also at Hanoi University of Science, Hanoi, Vietnam.
[w]Also at P.N. Lebedev Physical Institute, Russian Academy of Science (LPI RAS), Moscow, Russia.
[x]Also at Università di Roma Tor Vergata, Roma, Italy.
[y]Also at Università di Roma La Sapienza, Roma, Italy.
[z]Also at Università della Basilicata, Potenza, Italy.
[aa]Also at Università di Urbino, Urbino, Italy.
[bb]Also at Physics and Micro Electronic College, Hunan University, Changsha City, China.
[cc]Also at School of Physics and Information Technology, Shaanxi Normal University (SNNU), Xi'an, China.